JOURNAL OF MATERIALS SCIENCE 25 (1990) 3179–3185

Simultaneous measurement of contact angles and work of adhesion in metal–ceramic systems by the immersion–emersion technique

I. RIVOLLET, D. CHATAIN*, N. EUSTATHOPOULOS
Laboratoire de Thermodynamique et Physico-Chimie Métallurgiques, ENSEEG, BP 75, 38402 Saint Martin d'Hères Cédex, France

Comprehensive use of the immersion-emersion tensiometric method using a cylinder is proposed allowing simultaneous measurements of surface tension and contact angles in metal–ceramic systems. Tin and lead sapphire systems are investigated. Values measured for the surface tension of these metals are in accordance with that measured by the sessile drop method (σ_{LV}(Sn) = 465 ± 5 mJ m^{-2} at 1373 K and σ_{LV}(Pb) = 380 ± 5 mJ m^{-2} at 1193 K). Young's contact angles are evaluated from measured immersion and emersion contact angles and agree well with advancing contact angle measured by the sessile drop method (for Sn–Al_2O_3, θ_Y = 122° and θ_a = 122° at 1373 K, and for Pb–Al_2O_3, θ_Y = 121° and θ_a = 117° ± 3 at 1193 K). The effect of solid roughness on contact angle measurements is shown to be easily studied in metal–ceramic systems using the tensiometric method.

1. Introduction

Liquid metal–ceramic interfaces are becoming increasingly important in technology, especially in the production of metallic matrix composite materials and in the fields of brazing or pyrometallurgy. Moreover, the achievement of adequate mechanical, electrical and/or thermal properties of metal–ceramic materials greatly depends on the nature of the bonding between the two phases. The interactions between liquid metals and ceramics are macroscopically characterized by the work of adhesion, W_a, which is the energy per unit area, required to separate in a reversible way a solid from a liquid creating two surfaces (solid–vapour and liquid–vapour):

$$W_a = \sigma_{SV} + \sigma_{LV} - \sigma_{SL} \quad (1)$$

σ_{ij} are the interfacial tensions between two of the three phases: solid (S), liquid (L), vapour (V).

The expression for the contact angle, θ_Y, defined by Young from the vectorial equilibrium between the three interfacial tensions at the solid–liquid–vapour triple line is:

$$\cos \theta_Y = \frac{\sigma_{SV} - \sigma_{SL}}{\sigma_{LV}} \quad (2)$$

Then, the work of adhesion can be written as:

$$W_a = \sigma_{LV}(1 + \cos \theta_Y) \quad (3)$$

Knowledge of W_a requires the measurement of the surface tension of the liquid metal and the thermodynamic contact angle θ_Y. As in practice, the actual surface of the solid is never ideally chemically homogeneous and/or smooth, the measured contact angle, θ, is always different from θ_Y: when the liquid is advancing or receding on the solid, θ is respectively greater or smaller than θ_Y. Such a phenomenon results from the original defects of the solid surface and/or from other defects occurring during the contact between the liquid and the solid:

1. The adsorption–desorption of the liquid on the solid surface can momentarily influence the advancing and receding angles (θ_a and θ_r) and create a *molecular hysteresis* by changing σ_{SV} in front of the triple line.

2. Chemical heterogeneities of the solid surface can induce a chemical hysteresis due to local variation of σ_{SV} and σ_{SL}.

3. Lastly, the roughness of the solid can induce a topographical hysteresis by creating local barriers of mean slope δ (towards the apparent macroscopic surface) on which the triple line can stop when the liquid is advancing or receding on the solid.

As direct measurement of θ_Y is not possible, its value is often approached by the advancing angle on the more "ideal" surface (polished, monocrystalline, etc). Moreover, specific work on the hysteresis effect has been carried out to establish relations between θ_Y and θ_a and θ_r values [1–3].

The sessile drop method is the most classical method for measuring contact angles. Different techniques are used to produce advancing or receding angles, either by changing the volume of the drop or by tilting the substrate (see for example review [1]). But these devices are inconvenient when dealing with liquid metals, e.g. at high temperature, in a closed furnace under vacuum or controlled atmosphere. In this case, only the advancing contact angle is generally measured. Another method consisting in vertically displacing the solid toward the liquid is more suitable for these systems; it is known as

*Author to whom correspondence should be addressed.

0022–2461/90 $03.00 + .12

the wetting balance or tensiometric technique. The advancing (and receding) contact angle is obtained after the immersion (emersion) of the solid in (out of) the liquid. If the contact angle is less than 90°, it can be optically measured as the liquid meniscus formed around the solid is over the horizontal flat liquid surface. But if θ is higher than 90°, the tensiometric method is needed as it measures the weight of the meniscus which is proportional to the tension of adhesion T which is:

$$T = \sigma_{LV} \cos \theta \quad (4)$$

Knowing the surface tension of the liquid, θ can be measured [4] and, forcing the θ value to be zero or 180°, the surface tension also can be measured [5]. Such a tensiometric method has been widely used at low temperatures to measure the surface tension of organic and aqueous solutions, and to a lesser extent to determine contact angles. In the high temperature range, this technique was mostly used to determine interfacial tensions in metal–metal or metal–salt liquid–liquid systems [6, 7].

As our aim is the determination of W_a in metal–ceramic systems, σ_{LV} and θ have to be known. Of course, σ_{LV} values of many metals and alloys are already known [8, 9] but experimental conditions used for measuring this quantity can clearly differ from those used in θ measurements: indeed, in the temperature range where experiments are performed, contamination of the liquid can occur by atmospheric elements (oxygen for example) or slight dissolution of the crucible and of the actual solid under study. This contamination can induce significant changes in the surface tension of the liquid metal. So, to take into account such a phenomenon in W_a determination, a more comprehensive use of the "immersion–emersion method" is proposed allowing simultaneous measurement of the surface tension of the liquid and the contact angles. This involves measuring the variation in the tension of adhesion T as a function of the position of the triple line towards the horizontal flat liquid surface, e.g. the height of the meniscus, associated with a numerical resolution of the Laplace equation giving the shape of the surface of the meniscus formed around a vertical cylindrical solid of circular section.

Experiments with this method are performed in monocrystalline α-alumina–lead and tin, systems in which adsorption of the metal on the solid cannot occur [10]. On such substrates, only chemical and topographical hysteresis of the contact angle can be expected.

2. Immersion–emersion technique

2.1. Apparatus and experimental conditions

The apparatus which is described diagrammatically in Fig. 1 was designed with a view to using the immersion–emersion technique in liquid metals. The solid specimen is connected via a rod to one of the beams of a SETARAM 1012 electronic zero microbalance. As the weight of this charge is nearly counterbalanced by loading the other beam, the balance weights variations of masses from 1 g to 100 mg with an accuracy of 0.01%. The liquid is contained in a crucible of 50 to

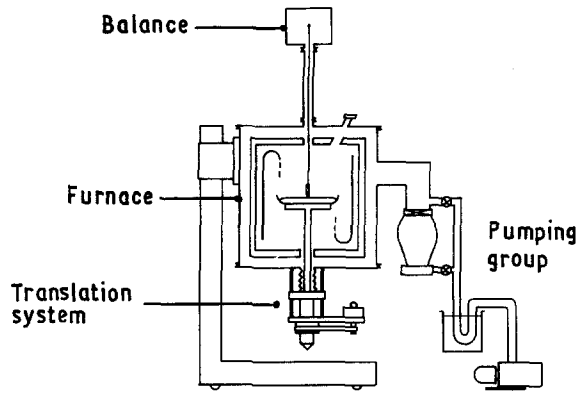

Figure 1 Sketch of the apparatus.

80 mm diameter, placed on a vertically mobile support. A synchronous motor controls the raising or lowering of this support at a constant speed from 10 to 10^{-2} mm min^{-1}. A molybdenum resistance heater allows a maximum temperature of 1873 K to be reached. Thermal insulations is achieved through molybdenum (internal) and steel (external) screens (the temperature of the liquid is measured by a Pt–Pt 10% Rh thermocouple located in the wall of the crucible). The water cooled double-wall stainless steel enclosure can be evacuated to 3×10^{-5} Pa by means of a rotary pump and an oil diffusion pump, or filled with neutral gas. Variations in the vertical force acting on the solid during its immersion and its emersion are recorded with time, e.g. with respect to the depth of immersion of the solid in the liquid as the speed of the translation of the liquid is constant and known.

The experiments with tin and lead were conducted with a graphite crucible under an atmosphere of helium which contains after purification on Al–Zr getter, oxygen at a partial pressure of about 10^{-16} Pa at 1000 K. The purity of the metals employed was 99.999%. The solid substrate consisted of cylinders (diameter 2.5 mm, length 30 mm) made of 99.993% pure monocrystalline α-alumina. Before the "immersion–emersion" experiment these solids were heat-treated at 1473 K for 1 h under vacuum in order to eliminate OH^- groups adsorbed on the surface [11]. The surface roughness parameters of the cylinders are measured on several generating lines with a TALYSURF 10. The as-received cylinders have a mirror-like polished surface. The value of the mean height R_a, and the mean wave length λ_a of the surface asperities are respectively 15 nm and 10 μm.

Different temperatures were explored beginning at the highest one when oxide films on the liquid metal surface can be eliminated by dissolution (for tin and lead [12]) or evaporation (for aluminium [13]). The last temperature step depends on the thermodynamic and kinetic conditions of reformation of these oxide films.

For comparison some wetting experiments were also conducted using the sessile drop method in an apparatus described elsewhere [12]. The plane substrates used have a surface roughness quality better than the cylinders. R_a is 5 nm and λ_a is less than 10 μm (the sensitivity limit of the roughness-meter). The materials and experimental conditions were identical to those just presented for immersion–emersion experiments,

except that the temperature steps were in increasing order because advancing contact angles are required.

2.2. Method

The immersion–emersion technique using cylindrical solids (of any cross-sectional shape) is presented in the case of non-wetting (Young contact angle greater than 90°) as it is the general case for non-reactive insulating ceramic–metal systems [14]. The case of wetting will be mentioned at the end of this section.

The force f exerted on a solid partially immersed in a liquid (base of the solid located at the level z with respect to the flat horizontal surface of the liquid) is equal to the sum of the weight of the solid in the gas (w_0), the weight of the liquid meniscus (w_m) with a joining angle ϕ and the buoyancy force:

$$f = w_0 + w_m + \Delta\rho g z s \quad (4)$$

$\Delta\rho$ is the difference in density between the liquid and the gas, g is the acceleration due to gravity, and s, the area of the base of the solid. Orr *et al.* [15] demonstrated that for a prism of any right section of perimeter p, the weight of the meniscus is:

$$w_m = \sigma_{LV} \cdot p \cdot \cos\phi \quad (5)$$

The curve of the variation in the force exerted on the solid during its immersion–emersion in the liquid as a function of the depth of immersion of the solid is shown diagrammatically in Fig. 2 with a number of successive positions of the solid in the liquid. As a convention, the origin of the force f is chosen as the weight w_0 of the solid in the vapour phase. It is shown that as the solid is immersed, it contacts the liquid (A) and the meniscus is progressively formed downwards (B) until the joining angle ϕ is equal to the immersion contact angle θ_i (C). Note that during this deformation of the liquid surface, the velocity of the solid–liquid–vapour triple line on the solid substrate, u, is strictly zero. From the point C, a deeper immersion of the solid does not give rise to any further change in the shape of the meniscus, the cylinder goes through the surface and the change in force is only due to the variation in the buoyancy force (C–D). During this phase, the triple line slips on the solid with a velocity $u = -v$, v being the immersion velocity of the solid with respect to the flat surface of the liquid. The emersion of the solid begins in D, the joining angle

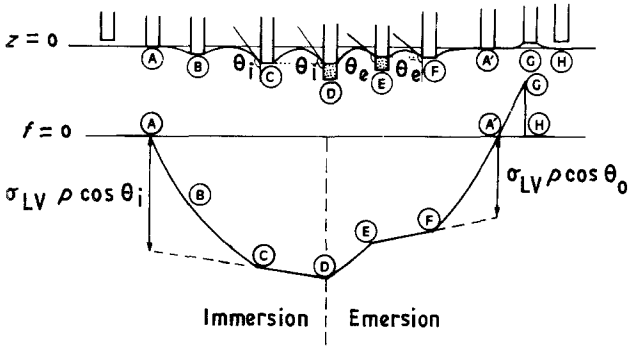

Figure 2 Common shape of an experimental curve of variation in the force exerted on a cylindrical solid during its immersion–emersion in a liquid as a function of the depth of immersion of the solid, in the non-wetting case.

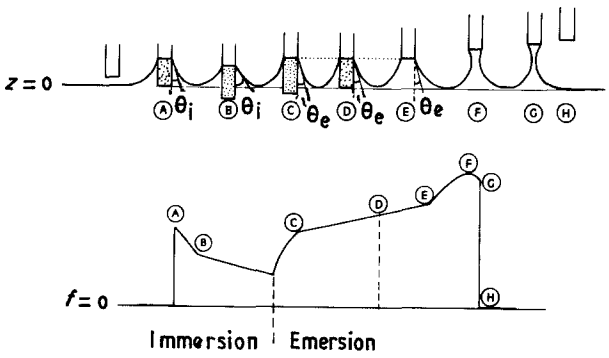

Figure 3 Common shape of an experimental curve of variation in the force exerted on a cylindrical solid during its immersion–emersion in a liquid as a function of the depth of immersion of the solid, in the wetting case.

changes continuously from θ_i to the emersion contact angle θ_e (D–E). The meniscus has an equilibrium shape from E to F and the change in force is only due to buoyancy. In F, the triple line is attached to the ridge of the base of the cylinder. From F to G, the joining angle changes from θ_e to ($\theta_e - 90°$) where the meniscus falls off the cylinder.

In the case of wetting (Young contact angle smaller than 90°) some differences appear as Fig. 3 shows. First, the advancing contact angle θ_a is spontaneously reached as soon as the solid touches the liquid. In this case, the speed of the triple line is not controlled but depends on the Young contact angle and the viscosity of the liquid: wetting occurs as in the sessile drop experiment, within about 10^{-3} sec [16]. Secondly when the solid is immersed the immersion contact angle $\theta_i > \theta_a$ is reached in B as in the non-wetting case. Another difference from the non-wetting case occurs at the end of the emersion of the solid: the joining angle of the liquid on the vertical solid surface goes through negative values (as shown in points F and G in Fig. 3). The joining angle corresponding to the breaking of the meniscus is θ_e–90° (with θ_e smaller than 90°). Consequently, the force exerted by the liquid on the solid goes through a maximum as a function of z. This maximum force can be used to determine directly the surface tension of the liquid phase [6].

From the non-linear parts of these curves (Figs 2 and 3) the surface tension of the liquid is determined. Then, from the intersection of linear and non-linear parts, the immersion and emersion contact angles are deduced. From Equations 4 and 5, at each point of the curve AC of Fig. 2 for example, the product $\sigma_{LV}\cos\phi$ is known (as f and z are measured). The other equation relating the three quantities σ_{LV}, ϕ and z is the Laplace equation:

$$\Delta P = \sigma_{LV}\left(\frac{1}{r_1} + \frac{1}{r_2}\right) \quad (6)$$

where ΔP is the pressure difference in and out of the liquid on each side of the surface and r_1 and r_2 the main curvature radii of the surface (see Fig. 4). In the case of a meniscus, ΔP is equal to the hydrostatic pressure and function of z:

$$\Delta P = \Delta\rho g z \quad (7)$$

Defining cross-sectional shape of the cylinder, r_1

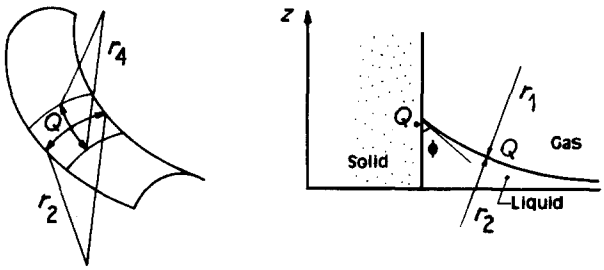

Figure 4 Geometrical quantities used to describe the liquid surface shape. (a) main curvature radii; (b) vertical position z of a point Q of the surface and joining angle ϕ of the liquid profile on the solid.

and r_2 are explicit functions of z, ϕ and their derivatives. Finally, a differential equation with the two variables z and ϕ can be written from Equations 6 and 7. This equation can be solved only in one case (if the solid is a blade with zero thickness) and a mathematical relation gives ϕ as a function of z and ϕ_{LV} [17]. However although the mathematical problem is solved, experiments with solids of blade shape are problematical! This is because the corners of the blade induce variations in the triple line level (see Fig. 5) and an erratic experimental curve $\sigma_{LV} \cos \theta = f(z)$ in comparison with the calculated curve using Equations 6 and 7. Experiments are in accordance with calculations only if the triple line level belongs to a plane perpendicular to the cylinder axis, e.g. if the solid is a vertical cylinder of circular section.

In Fig. 6, the geometrical quantities used to describe the profile of a meniscus formed on a circular and constant-section of a cylinder are plotted. Using the cartesian coordinates, the Laplace equation is written:

$$\mathrm{d}(x \sin \alpha)/\mathrm{d}x = \left(-\frac{\Delta\rho g}{\sigma_{LV}}\right) zx \qquad (8)$$

Like Hartland and Hartley [17], the differential equation was numerically solved, adapted to the form of the experimental information available: successive $\sigma_{LV} p \cos \phi = f(z)$ curves are calculated for different σ_{LV} values between $\phi = 90$ and 180° and compared with the experimental one obtained with a cylinder of perimeter p. σ_{LV} is determined from the calculated curve which has the best coincidence with the experimental one. The program used for the calculations is presented elsewhere [18]. Once σ_{LV} is known, θ_i and θ_e can be determined from the forces measured in point C and E (Fig. 2) corrected for the buoyancy forces (dashed lines) as they give $\sigma_{LV} p \cos \theta_i$ and $\sigma_{LV} p \cos \theta_e$ (see Fig. 2).

3. Experiments

3.1. Some experimental remarks on non-wetting systems

3.1.1. Effect of the ridge at the base of the cylinder

Theoretically, when the solid is immersed, the liquid surface is bent until the joining angle reaches θ_i. Joining angles ϕ greater than θ_i are in fact momentarily observed, as the triple line is blocked by the particular roughness of the ridge of the cylinder. When the liquid passes through this ridge, the triple line is located on the generating line of the cylinder, the meniscus shape changes to find its equilibrium and the joining angle decreases to θ_i. This phenomenon is shown on Fig. 7 (left side) and corresponds to a minimum force at the point C of Fig. 2. The difference between the maximum joining angle, ϕ_{max}, and θ_i is just a few degrees. To prevent this ridge effect, the immersion contact angle, θ_i, has to be measured during a second immersion begun with a triple line located on the generating lines of the cylinder as shown on the right hand side of Fig. 7.

3.1.2. Effects of the solid translation speed

During an immersion–emersion experiment, three types of contact angle can be observed. On Fig. 8, these angles are shown and referenced by two superscripts: the first superscript is the velocity of the triple line with respect to the solid, and the second is the velocity of the solid with respect to the flat surface of the liquid (the subscript is always, i or e, describing the direction of motion of the solid in the liquid).

$\theta^{0,v}$ is the contact angle measured on the non-linear part of the experimental curves at the point where the calculated meniscus weight-meniscus height curve ($\sigma_{LV} p \cos \phi = f(z)$) diverges from the experimental one. From this point, the triple line begins to move on the solid in order to reach *continuously* a velocity equal to $-v$.

$\theta^{-v,v}$ is the stationary contact angle reached when the triple line is slipping perfectly on the solid, i.e. the

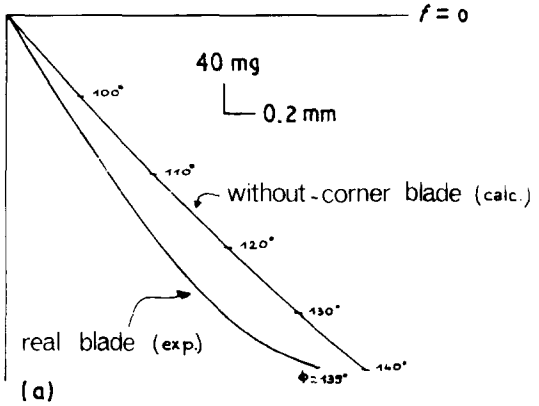

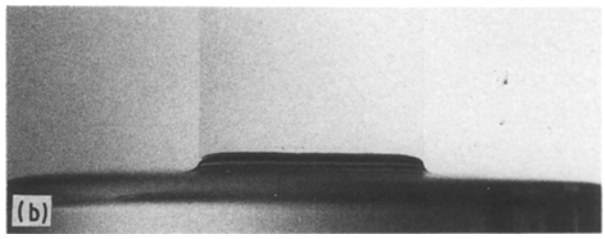

Figure 5 (a) Erratic meniscus weight–meniscus height experimental curve for a blade in the Hg–sapphire system due to the different level of the triple line near the corners of the blade. (b) a photograph of this phenomenon for water on glass ($\theta_Y < 90°$) at 300 K in air.

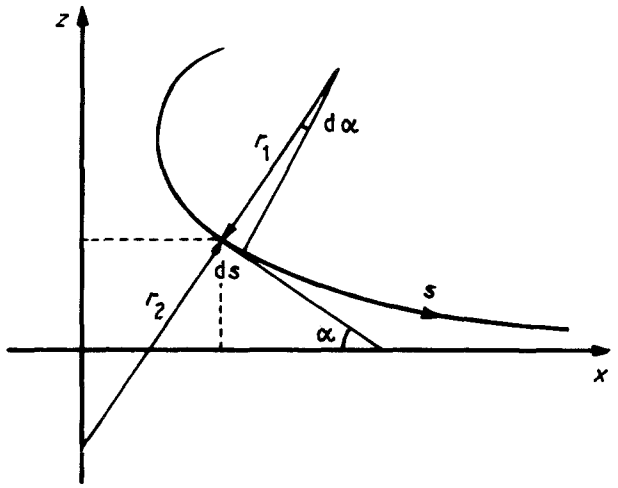

Figure 6 Geometrical quantities used to describe the profile of a meniscus formed around a circular and constant section cylinder.

triple line stays at the same distance from the flat horizontal surface of the liquid. This contact angle is measured at the intersection of the calculated extension of the $\sigma_{LV}p \cos \phi = f(z)$ curve (the dashed line) with the straight line just following corresponding to the variation in the buoyancy force.

A third contact angle $\theta^{0,0}$ can be measured after stopping the motion of the solid, when the velocity of the triple line (initially equal to $-v$) becomes zero on the motionless solid: this is a static contact angle.

It is known [19] that contact angle values depend on the velocity of the triple line. In many non-wetting systems with substrate roughness R_a varying by a factor of 10^3 (Al_2O_3–Sn, glass–Hg) [18] it was found that the difference between $\theta^{-v,v}$ and $\theta^{0,v}$ is about 5° at 10^{-2} mm min^{-1} velocity in the following order:

$$\theta_i^{-v,v} > \theta_i^{0,v}$$

and

$$\theta_e^{-v,v} < \theta_e^{0,v}$$

Moreover, the difference between $\theta^{0,v}$ and $\theta^{-v,v}$ did not change as the speed was increased up to 1 mm min^{-1}.

Another observation worth mentioning is the very close values (within the experimental error of the measurements) of $\theta^{0,v}$ and $\theta^{0,0}$ regardless of the speed used (from 10^{-2} to 1 mm min^{-1}). For example, results

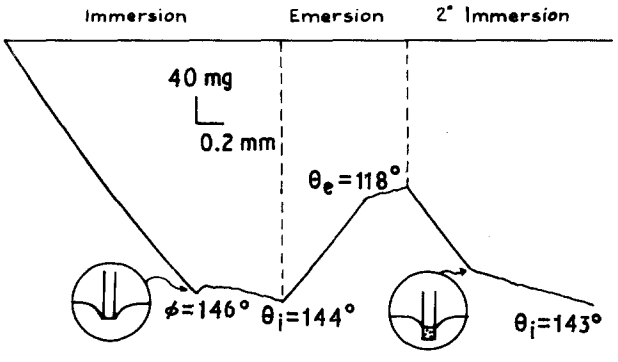

Figure 7 Observation of a minimum force due to the ridge at the base of the solid in the Sn–sapphire system at 1373 K.

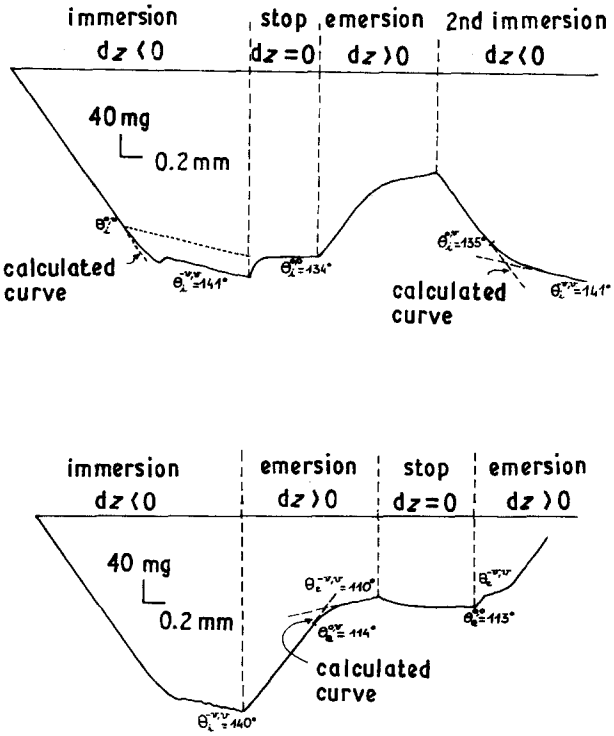

Figure 8 The three types of contact angles observed during an immersion-emersion experiment in the Sn–sapphire system at 1373 K.

for Sn–Al_2O_3 can be seen on Fig. 8. From this observation, it can be concluded that equilibrium contact angles can be obtained from dynamic immersion–emersion experiments in the velocity range proposed. Consequently the contact angle will be noted θ^0 hereafter regardless of whether it is $\theta^{0,0}$ or $\theta^{0,v}$.

3.2. Results and discussion

3.2.1. Surface tension

Experimental values obtained for surface tensions of tin and lead are presented in Table I in comparison with recent determinations by Nogi *et al.* [20] using the sessile drop method. Note that our values are slightly smaller (2.5%) but this difference is typical of the dispersion of surface tension values measured by different authors and/or different methods.

The temperature coefficient $d\sigma_{LV}/dT$ has the correct sign and order of magnitude ($\simeq -0.1$ mJ m^{-2} K^{-1}) but the temperature range explored is too small to propose precise values of this quantity.

The accuracy on σ_{LV} measurements by this immersion–emersion method is about 1% taking into account the errors due to apparatus, and the reproducibility is $\pm 3\%$ at a given temperature for two independent experiments. This experimental error is the same as that made in determining the surface tension of metals

TABLE I

	T (K)	σ_{LV} (mJ m^{-2})	σ_{LV} [20] (mJ m^{-2})
Sn	1273	475 ± 5	482
	1373	465 ± 5	473
Pb	1023	390 ± 5	399
	1193	380 ± 5	381

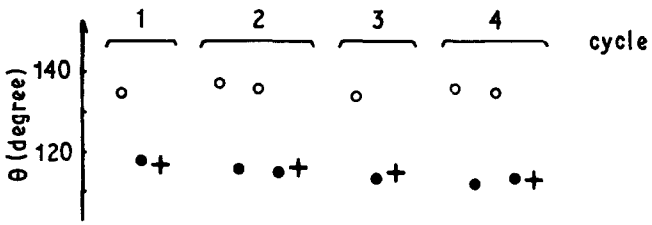

Figure 9 Reproducibility of θ_i^0 measurements of tin on sapphire at 1373 K during successive immersion–emersion cycles. Points repered by + are θ_e^0 values measured at the breaking of the meniscus.

by the sessile drop method [9]. Clearly, the inconvenience of the immersion–emersion method in determining σ_{LV} is the quantity of liquid metal necessary for the experiments (more than 20 cm^3) but in the case of cheap metals or alloys, it is balanced by the drop symmetry problems of the sessile drop method.

3.2.2. Contact angles

The error in contact angle measurements due to (i) the precision of the balance, (ii) the translation system of the crucible and (iii) the recorder, is estimated to be less than 0.5°.

Fig. 9 shows the reproducibility of θ_i^0 and θ_e^0 measurements of tin on sapphire during successive immersion–emersion cycles, the contact line being located at an increasingly greater distance from the base of the cylinder. Contact angles are reproducible within $\pm 3°$ as in two experiments with two cylinders. This shows the homogeneity of the topological and "chemical" roughness (the chemical roughness is a small-scale chemical heterogeneity as defined by Joanny and de Gennes [3]). Moreover, considerable hysteresis ($\theta_i^0 - \theta_e^0$) is observed which may be due either to one of the two types of roughness or to both of them. However, complementary experiments performed with solids of $R_a < 5$ nm [21] show that when the roughness tends towards zero, the hysteresis of the contact angle ($\theta_i^0 - \theta_e^0$) also tends towards zero. This would show that the chemical roughness has no effect. For contact angle hysteresis of this type the Young contact angle can be calculated from θ_i^0 and θ_e^0 values using [18, 21]:

$$\theta_Y = Arcos\left(\frac{\cos\theta_i^0 + \cos\theta_e^0}{2r}\right) \quad (9)$$

where r is the Wenzel parameter, i.e. the ratio of the true area of the rough surface to the geometrical area.

Table II shows several values of contact angle measured on tin–sapphire and lead–sapphire systems. There are immersion and emersion contact angles (θ_i^0 and θ_e^0) determined by the tensiometric method described here using cylinders with a mean slope of surface asperities (R_a/λ_a) of 0.0015. Advancing contact angles (θ_a) determined by the sessile drop method on substrates of R_a/λ_a of 0.0005 are also shown in Table II. These values come from a previous study [12] for the tin–sapphire system. Advancing contact angles for the lead–sapphire system were determined for this study by the sessile drop method between 723 and 1173 K, and are shown on Fig. 10. The line giving the contact angle as a function of temperature is written:

$$\theta_a(Pb) = 125 - 0.014(T - T_m^{Pb}) \quad (10)$$

where T_m^{Pb} is the melting temperature of lead.

The third type of θ values presented in Table II are the θ_Y values calculated from θ_i^0 and θ_e^0 values using Equation 9.

It may come as a surprise to find that θ_i^0 values are much greater than θ_a values whereas the substrate roughness, and particularly the mean slope of the surface asperities R_a/λ_a of the cylinder and the plane substrate, are very similar. Moreover, taking into account the experimental error, θ_a values are equal to the calculated values of θ_Y. These results agree with those of Hitchcock *et al.* [24] which show that roughness has a negligible effect on the advancing contact angle measured by the sessile drop method if R_a/λ_a is less than 0.005. All these results in metal–ceramic systems can be understood if consideration is given to the way in which they are obtained: using the immersion–emersion technique, θ_i^0 is reached reversibly as the triple line does not move on the solid while in the case of the sessile drop method, θ_a is reached irreversibly as the triple line is moving spontaneously on the solid. Huh and Mason [23] explain that part of the kinetic energy of the liquid drop (acquired at the beginning of spreading) is used to jump the barriers constituted by the asperities of the solid surface.

If the real shape of the surface is taken into account, a mean value of R_a/λ_a of 0.0015 can correspond to a maximum value of R/λ of about 10° [18]. Then, θ_i^0 values approach the maximum value of the advancing contact angle which is $\theta_Y + (R/\lambda)_{max}$ [25]. The reversible way in which θ_i^0 and θ_e^0 values are reached by the immersion–emersion method would provide a means of approaching the maximum value of the contact angle hysteresis due to the topographical roughness in metal–ceramic systems. The maximum value can never be attempted because of the intrinsic vibrations of the apparatus.

A final remark can be made concerning the same amplitude of the hysteresis found for tin and lead on

TABLE II

System	T (K)	θ_a (deg)	θ_i^0 (deg)	θ_e^0 (deg)	θ_y (deg)	$\theta_i^0 - \theta_e^0$ (deg)
Sn/Al_2O_3	1373	122 ± 2	136 ± 2	114 ± 3	122	22
Pb/Al_2O_3	1023	119 ± 3	133 ± 1	115 ± 1	123.5	18
	1193	117 ± 3	131 ± 2	112 ± 2	121	16

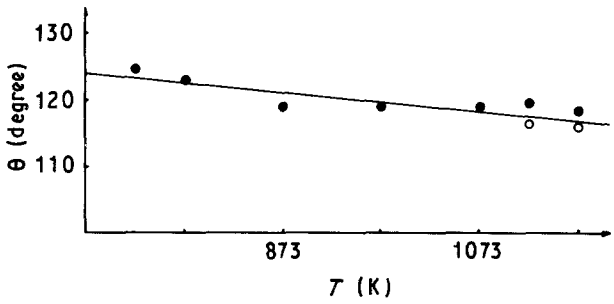

Figure 10 Variation with temperature of contact angle of lead on sapphire in Ar 5%H_2 atmosphere.

sapphire substrate of same roughness. This may be due to the similarity of the bulk and surface thermodynamic quantities (σ_{LV}, θ_Y) of these two metals. The authors are currently studying the effect of these different parameters on the width of the contact angle hysteresis in metal–sapphire systems.

4. Conclusions

In this version of the tensiometric method, surface tension and contact angles can be simultaneously measured and, consequently, the work of adhesion in metal–ceramic systems can be estimated in self-consistent conditions. In this work the method has been successfully used for tin and lead–sapphire systems.

The accuracy of the surface tension values is good compared with that measured by the sessile drop method, but the latter method is easier.

The immersion–emersion method is interesting for practical studies on the wettability of fibres or monofilaments used in metal matrix composites [16]. Moreover, this method is particularly suitable for studying the effect of roughness on the wetting of liquid metals on refractory solids.

Acknowledgement

This work was supported by CNES.

References

1. R. E. JOHNSON and R. H. DETTRÉ, *Surface Coll. Sci.* **2** (1969) 85.
2. J. D. EICK, R. J. GOOD and A. W. NEUMANN, *J. Colloid Interface Sci.* **53** (2) (1975) 235.
3. J. F. JOANNY and P. G. de GENNES, *J. Chem. Phys.* **81** (1) (1984) 552.
4. J. CHAPPUIS and J. M. GEORGES, *J. Chim. Phys.* **71** (1974) 567.
5. F. VERGARA and B. LESPINASSE, Bulletin de la Société Chimique de France (1970) p. 3227.
6. D. CHATAIN, L. MARTIN-GARIN and N. EUSTATHOPOULOS, *J. Chim. Phys.* **79** (1982) 569.
7. L. MARTIN-GARIN, A. DINET and J. M. HICTER, *J. Mater. Sci.* **14** (1979) 2366.
8. L. D. LUCAS, Techniques de l'Ingenieur, Paris, M67, (1984) p. 1.
9. N. EUSTATHOPOULOS and J. C. JOUD, "Current Topics in Materials Science", Vol. 4, edited by E. Kaldis (North Holland, 1980) p. 281.
10. P. NIKOLOPOULOS, *J. Mater. Sci.* **20** (1985) 3993.
11. J. J. BRENNAN and J. A. PASK, *J. Amer. Ceram. Soc.* **51** (1968) 569.
12. I. RIVOLLET, D. CHATAIN and N. EUSTATHOPOULOS, *Acta Metall.* **35** (1987) 835.
13. V. LAURENT, D. CHATAIN, C. CHATILLON and N. EUSTATHOPOULOS, *Acta Metall.* **36** (1988) 1797.
14. D. CHATAIN, L. COUDURIER and N. EUSTATHOPOULOS, *Rev. Phys. Appl.* **23** (1988) 1055.
15. F. M. ORR Jr, L. E. SCRIVEN and T. Y. CHU, *J. Colloid Interface Sci.* **60** (1977) 402.
16. V. LAURENT, Thesis, INP Grenoble (1988).
17. S. HARTLAND and R. W. HARTLEY, "Axisymmetric Fluid-Liquid Interfaces", (Elsevier, Amsterdam, 1976).
18. I. RIVOLLET, Thesis, INP Grenoble (1986).
19. E. B. DUSSAN, *Ann. Rev. Fluid. Mech.* **11** (1979) 371.
20. K. NOGI, K. OGINO, A. C. McLEAN and W. A. MILLER, *Met. Trans.* **17B** (1986) 163.
21. V. DE JONGHE, D. CHATAIN, I. RIVOLLET and N. EUSTATHOPOULOS, *J. Chim. Phys.* in press.
22. J. CHAPPUIS, "Multiphase Science and Technology", Vol. I, edited by G. F. Hewitt, J. M. Delhaye and N. Zuber (McGraw Hill, 1984) p. 387.
23. C. HUH and S. G. MASON, *J. Colloid Interface Sci.* **60** (1977) 11.
24. S. J. HITCHCOCK, N. T. CARROLL and M. G. NICHOLAS, *J. Mater. Sci.* **16** (1981) 714.
25. R. SHUTTLEWORTH and G. L. J. BAILEY, *JCS Discussions Faraday Soc.* **3** (1948) 16.

Received 13 March
and accepted 30 August 1989